Trinuclear Ni(II) Complex with Rare Deprotonation of the Bridging Oxamate and Imino Nitroxide Radical as Blocking Ligand

Vitaly A. Morozov , Denis G. Samsonenko , Kira E. Vostrikova *

Posted Date: 30 May 2025

doi: 10.20944/preprints202505.2369.v1

Keywords: nickel(II); tri-nuclear complex; imino nitroxide; bis-oxamate ligand; N,N′-1,4-phenylenebis(oxamate); 2-(6-methyl-2-pyridyl)-4,4,5,5,5-tetramethylimidazoline-1-oxyl

 doi:10.20944/preprints202505.2369.v1

Article

Trinuclear Ni(II) Complex with Rare Deprotonation of the Bridging Oxamate and Imino Nitroxide Radical as Blocking Ligand

Vitaly A. Morozov [1], Denis G. Samsonenko [2] and Kira E. Vostrikova [2,*]

[1] International Tomography Center SB RAS, Institutskaya Str. 3a, 630090 Novosibirsk, Russia

[2] Nikolaev Institute of Inorganic Chemistry SB RAS, 3 Lavrentiev Avenue, 630090 Novosibirsk, Russia

* Correspondence: vosk@niic.nsc.ru

Abstract: Phenylene-based bis-oxamate polydentate ligands offer unique opportunities for creating a large variety of coordination compounds in which paramagnetic metal ions are strongly magnetically coupled. The employment of iminonitroxyl (IN) radicals as supplementary ligands confers numerous benefits, including the strong ferromagnetic interaction between Ni and IN. Furthermore, the chelating IN can function as a blocking ligand, thereby impeding the formation of coordination polymers. In this study, we present the molecular, crystal structure, experimental, and theoretical magnetic behavior of an exceptional neutral trinuclear complex $[Ni(L^{3-})_2(IN)_3]\cdot 5MeOH$ (**1**) with a cyclic triangular arrangement. Moreover, in this compound three Ni^{2+} ions are linked by the two bis-oxamate ligands playing rare tritopic function due to an unprecedented triple deprotonation of the related meta-phenylene-bis(oxamic acid). Despite the presence of six possible magnetic couplings in the three-nuclear cluster **1**, its behavior was reproduced well using a three-***J*** model and ZFS, under the assumption that the three different Ni-IN interactions are equal to each other, whereas only two equivalent in value Ni-Ni interactions are taken into account, and the third one was equated to zero. These studies indicate the presence of two opposite in nature type of magnetic interactions within triangular core. DFT and CASSCF/NEVPT2 calculations were completed to support the experimental magnetic data simulation.

Keywords: nickel(II); tri-nuclear complex; imino nitroxide; bis-oxamate ligand; *N,N'*-1,4-phenylenebis(oxamate); 2-(6-methyl-2-pyridyl)-4,4,5,5,5-tetramethylimidazoline-1-oxyl;

1. Introduction

Polytopic organic ligands [1] of different topology are used for creating metallo-supramolecular assemblies with variable structural and physical properties. Bis-oxamate phenylene-based polydentate ligands offer a unique potential for a greater variety of coordination compounds, both homo- and heterometallic, in which spin-bearing metal ions are strongly magnetically coupled [2–6]. Despite a thirty-year history of studying such systems, no polynuclear complex in which N,N'-1,4-phenylenebis-oxamic acid (L) was triple-deprotonated (L^{3-}) (Figures 1a and 1b) has yet been identified. In previous studies, the synthesis of compounds with half-deprotonated (L^{2-}) [6–10] and fully deprotonated ligand (L^{4-}) [11–20] (Figures 1c and 1e respectively) has been achieved. In addition, it has been shown that nickel(II) complexes in a distorted coordination octahedral environment can possess both optical and magnetic properties necessary for their use as quantum qubits [21,22].

The utilization of imino nitroxyl (IN) radicals as supplementary ligands confers several advantages. Firstly, it is a blocking function to prevent the formation of coordination polymers. Secondly, it has been established that, in contrast to nitronyl nitroxyl (NN) radicals, which exhibit strong antiferromagnetic coupling in Ni-NN pair [23–26], the Ni-IN interaction is ferromagnetic and strong [23,27–36]. The latter circumstance is of significant importance from the standpoint of enhancing the full spin value of the molecular cluster.

 doi:10.20944/preprints202505.2369.v1

In this paper, we present the molecular, crystal structure, experimental and theoretical magnetic behavior of an exceptional neutral trinuclear complex $[Ni(L^{3-})_2(IN)_3]\cdot 5MeOH$ (**1**) having a cyclic triangular arrangement, where IN is an imino nitroxyl radical, 2-(6-methyl-2-pyridyl)-4,4,5,5-tetramethylimidazoline-1-oxyl (Figure 1f). Moreover, in this compound three Ni^{2+} ions are linked by the two bis-oxamate ligands playing rare tritopic function due to an unprecedented triple deprotonation of the related meta-phenylene-bis(oxamic acid).

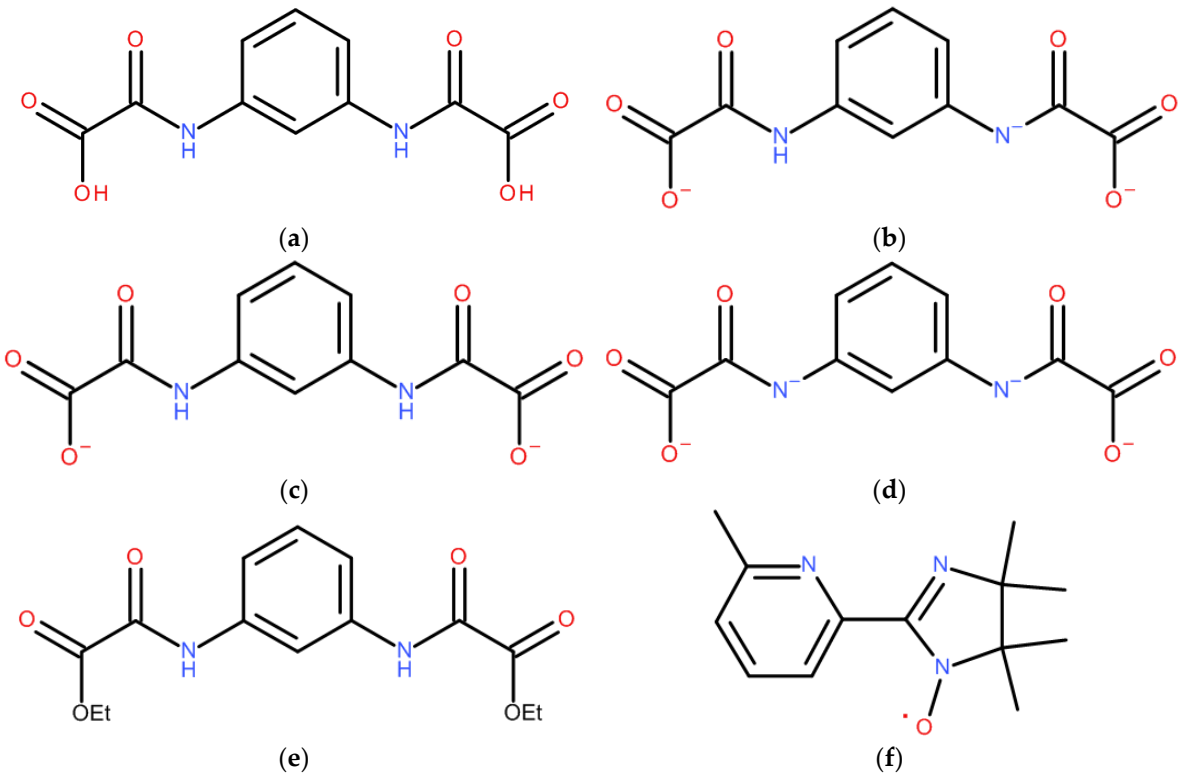

Figure 1. Organic entities pointed out in the text with their IUPAC names : (**a**) 2- [3-(oxaloamino)anilino]-2-oxo-acetic acid; (**b**) 2- [3-(carboxylatoformyl)azanidylanilino]-2-oxo-acetate; (**c**) 2- [3-[(carboxylatoformyl)amino]anilino]-2-oxo-acetate; **(d)** 2- [3-(carboxylatoformyl)azanidylphenyl]azanidyl-2-oxo-acetate ; (**e**) ethyl-2- [3- [(2-ethoxy-2-oxo-acetyl)amino]anilino]-2-oxo-acetate; (**f**) 2-(6-methyl-2-pyridyl)-4,4,5,5-tetramethylimidazoline-1-oxyl.

2. Results and Discussion

2.1. Synthesis and Characterization

Two aqueous solutions, 1 and 2, were prepared simultaneously under agitation on magnetic stirrers at 80 °C. The utilized starting materials and their respective quantities are delineated in section 3.3.1. Solution 1 contained bis-oxamate ligand coordinated to the metal, while solution 2 contained the chelate complex $[Ni(IN)(H_2O)_4]^{2+}$. Solution 2 was added dropwise to solution 1 without removing the heating. Following the heating and cooling stirring procedures, which were each 15 minutes in duration, the resultant red-orange precipitate was filtered through a porous glass filter. The precipitate was then washed with a small amount of water and dried on the filter until it became friable, while sucking in air. The solid was then dissolved in 5 mL of hot methanol. After filtering, the product solution was left undisturbed for several days. The dark red crystals that formed were used for structure determination. It is well established that crystals of the complex quickly lose solvate molecules when stored in air. For further characterization, we used either freshly prepared crystals (TG and IR) or powder brought to constant weight by heating at 80°C (elemental analysis).

In Supplementary Materials (SM) the results of the FTIR spectral and thermogravimetric investigations of $[Ni_3(L^{3-})_2(IN)_3]\cdot 5CH_3OH$ (**1**) are presented. The thermic study of 1 is illustrated in

 doi:10.20944/preprints202505.2369.v1

Figure S1, SM. After loss of solvated methanol molecules in the range of 20-100°C (theoretical mass loss is 10.46 %), the solid phase of three-nuclear cluster is thermally stable up to 210°C. After reaching a steady weight, dry complex $[Ni(L^{3-})_2(IN)_3]$ was further heated to 360°C. At that final temperature, the mass loss was 55.15% of the initial mass. This result supports the assumption that the final product in this experiment was probably nickel(II) carbonate.

IR spectrum of **1** confirms (Figure S2, SM) the absence of perchlorate ions from starting nickel salt, indicating the neutrality of the cluster. The vibrations due to the participation of solvated alcohol molecules in the hydrogen bonding system create an intense and broad band in the 3750-2700 cm^{-1} region (ν_{max}=3400 cm^{-1}), covering also the absorption bands from >N−H (shoulders at 3268 and 3102 cm^{-1}) and C−H (2965, 2925 and 2857 cm^{-1}) from the methyl groups of IN. An intense asymmetric absorption band in the 1800–1500 cm^{-1} region with a maximum at 1590 cm^{-1} covers few vibrations: shoulder at 1717 cm^{-1} of (C=O), band at ~1656 cm^{-1} of $(O-C=O)_{asym}$ and the C=C and C=N stretching vibrations. The two peaks at 1448 cm^{-1} and 1335 cm^{-1} apparently correspond to $\nu(C-N_{Py})$ and C=O vibrations respectively. The other absorptions can be assigned to: a symmetric mode of O−C=O at 1472 cm^{-1}, a shoulder at 1386 cm^{-1} to ν(N−O), at 1072 and 700 cm^{-1} to δC−H in-plane and δC−H out-of-plane respectively. The other less intense absorption bands in 1200−400 cm^{-1} area predominantly belong to IN ligand.

2.2. Crystal and Molecular Structure

The crystal structure of **1** contains trinuclear molecular clusters of $[Ni_3(L^{3-})_2(IN)_3]$ and solvate methanol molecules. It has been established that each Ni^{2+} cation coordinates an imino nitroxide (IN) paramagnetic ligand in a chelate manner. $\{Ni(IN)\}^{2+}$ fragments are interlinked with two *m*-phenylene-bis(oxamate) anions, L^{3-}, to form trinuclear complex, Figure 2.

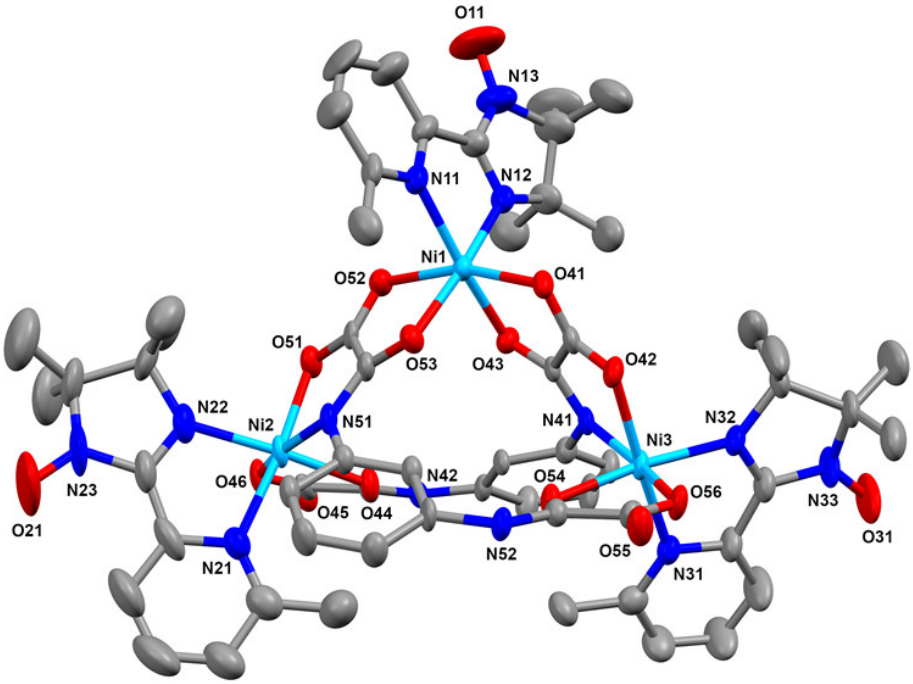

Figure 2. Structure of $[Ni_3(L^{3-})_2(IN)_3]\cdot 5MeOH$ (**1**). H atoms are omitted, ellipsoids of 50% probability.

All the metallic centers are situated within a distorted octahedral coordination environment. Ni1 one is linked with two nitrogens atoms of the radical ligand (N11, N12) and four oxygen atoms of two L^{3-} anions (O41, O43, and O53, O53). Both Ni2 and Ni3 cations possess an identical coordination environment, comprising three N atoms of an IN ligand (N21, N22 for Ni2, and N31, N32 for Ni3) and an L^{3-} anion (N51 for Ni2 and N41 for Ni3). In addition, the coordination environment incorporates three O atoms of two L^{3-} anions (O44, O46, O51 for Ni2, and O54, O56, O42 for Ni3),

 doi:10.20944/preprints202505.2369.v1

which are linked in a *fac* manner. Ni–N and Ni–O bond lengths and valence angles are listed in the Table S2 (Supplementary Material, SM). As demonstrated in Table S3, the coordination environment of each Ni ion is a distorted octahedron. The matching ratios are very close for Ni1 and Ni2, and the ratio for Ni3 slightly exceeds them. The arrangement of the triangle molecules along the *c* axis gives rise to the formation of a supramolecular chain. In the latter, each complex is connected with adjacent molecules by means of hydrogen bounding between −N–H (N42 and N52) and O=C− (O45 and O55) groups of two L^{3-} ligands (Figure 3) with the N…O distances of 2.795(5) and 2.829(5) Å. Interactions between neighboring chains are established via CH···O contacts between the pyridyl −CH group (C103) of the radical and the coordinated oxygen atom (O46) of the L^{3-} anion. These results in the formation of a wave-shaped supramolecular layer that is oriented parallel to the *bc* plane (Figure S3, SM) with the N…O distance of 3.182(8) Å. The layers exhibit an alternating pattern along crystallographic axis *a*. The structure contains 28% solvate accessible void volume, which was estimated with PLATON [37]. This volume is occupied by guest methanol molecules. The latter form a system of hydrogen bonds, which involves CH_3OH···$HOCH_3$ and CH_3OH···O(L^{3-}) contacts, the O…O distances being in range 2.48(3)–2.851(6) Å.

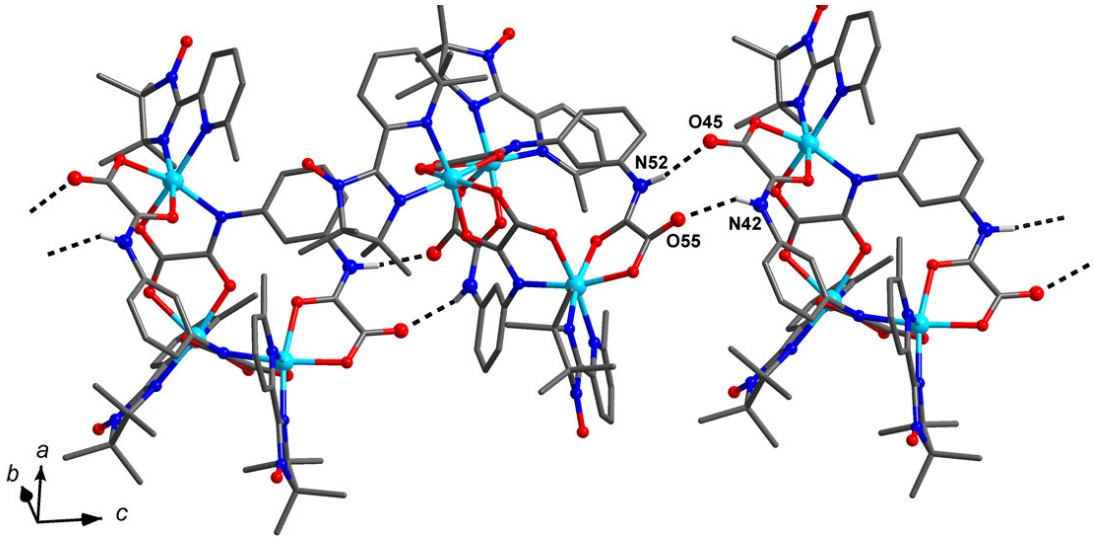

Figure 3. Fragment of supramolecular chain in the structure of **1** (H atoms are omitted; H-bonds are shown with dashed lines).

2.3. Magnetic Studies

2.3.1. Cryomagnetic measurements

The temperature dependence of susceptibility for a polycrystalline sample of **1** is presented in Figure 4 as a χT *vs* T graphic. The room temperature χT value (4.93 emu K mol^{-1}) is closed to the value corresponding to the sum uncorrelated spins of constituent paramagnetic centers. As the temperature decreases to 2 K, the χT value steadily decreases, indicating the predominance of antiferromagnetic interactions in the solid phase of the compound. This is also shown by the field dependence data of the magnetization (Figure 5), as the value of M(H) at H = 7 T is only 3.26 μ_B.

In the context of AC magnetic measurements conducted at temperatures below 25 K, no significant correlation was identified between the magnetic susceptibility and the field oscillation frequency, irrespective of the presence or absence of an external magnetic field with a strength of B = 0.1 T.

 doi:10.20944/preprints202505.2369.v1

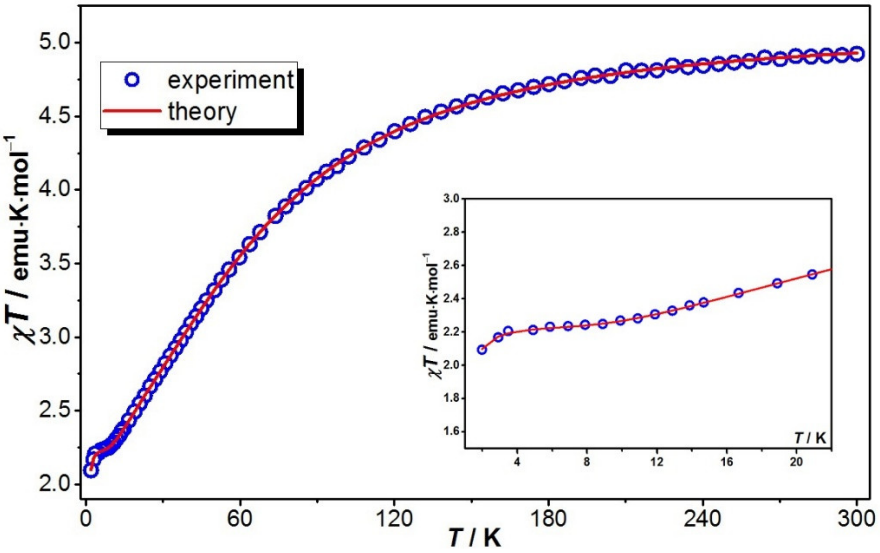

Figure 4. Temperature dependence of the χT product at B = 0.25 T. The solid lines represent the theoretical simulation to the experimental data (open circles).

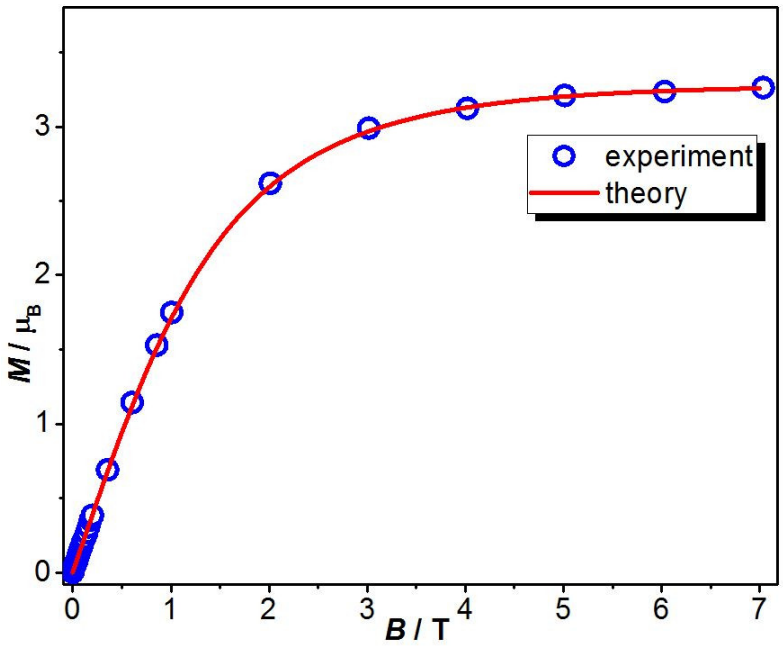

Figure 5. The magnetization curve measured for **1** at 2.8 K. The solid line represents the theoretical simulation to the experimental data (open circles).

2.3. Magnetic Behavior Modeling and Theoretical Calculations

2.3.1. Theoretical Model and Exhaustive Parameter Set Required for Magnetic Data Simulation

Theoretical modeling of the magnetic behavior of the investigated complex, considering two different types of magnetic coupling (Scheme 1), was performed using the expression for the spin-Hamiltonian (SH) outlined below

$$\begin{aligned}\hat{H} = &-2J_1\hat{S}_{M1}\cdot\hat{S}_{R1} - 2J_2\hat{S}_{M2}\cdot\hat{S}_{R2} - 2J_3\hat{S}_{M3}\cdot\hat{S}_{R3} - \\ &-2J_{11}\hat{S}_{M1}\cdot\hat{S}_{M2} - 2J_{12}\hat{S}_{M1}\cdot\hat{S}_{M2} - 2J_{13}\hat{S}_{M2}\cdot\hat{S}_{M3} + \\ &+\hat{S}_{M1}\boldsymbol{D}_1\hat{S}_{M1} + \hat{S}_{M2}\boldsymbol{D}_2\hat{S}_{M2} + \hat{S}_{M3}\boldsymbol{D}_3\hat{S}_{M3} + \\ &+g_{Ni}\beta(\hat{S}_{M1}+\hat{S}_{M2}+\hat{S}_{M3})\cdot B_0 + g_R\beta(\hat{S}_{R1}+\hat{S}_{R2}+\hat{S}_{R3})\cdot B_0\end{aligned}$$

The initial line of the expression delineates the exchange interaction between nickel ions (M_n) and the IN-radicals (R), while the subsequent line accounts for the M-M exchange interaction. The

 doi:10.20944/preprints202505.2369.v1

third and fourth lines represent the zero-field splitting (ZFS) for Ni^{2+} -centers having S = 1 and the Zeeman interaction with the external magnetic field B_0, respectively. In order to circumvent the over-parameterization problem, the isotropic g-factor for nickel (g_M) was utilized, and the value of g_R was assumed to be 2.

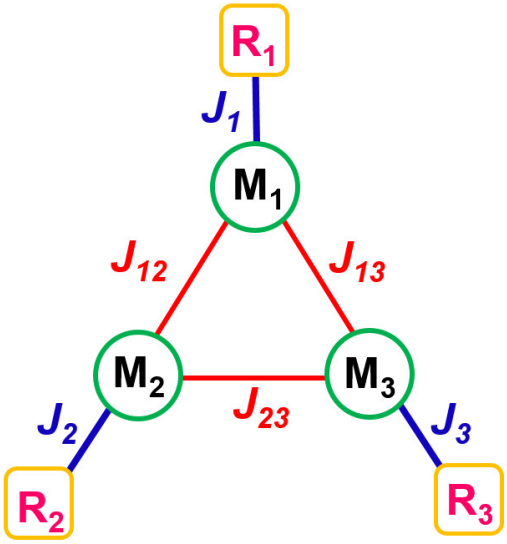

Scheme 1. Topological structure of magnetic exchange interactions between spin carriers in complex **1**: M_n = Ni_1, Ni_2 and Ni_3, R_n = IN radical coordinated to the corresponding Ni-center.

The results of DFT calculation of exchange integrals by broken symmetry (BS) method using different functionals are summarized in Table 1. The latter shows that the nickel-radical magnetic couplings (J_1, J_2, J_3) are roughly the same within a method and ferromagnetic (FM), whereas the metal-metal interaction in M_1–M_2 and M_1–M_3 pairs are has the opposite sign. Hybrid functionals (B3LYP and TPSSh) give about one and a half times larger coupling values than the more recent range-separated DF variants. A separate calculation using the B3LYP method also showed that the exchange integral J_{12} between spins Ni_2 and Ni_3 is small and does not exceed 0.05 cm^{-1}. Therefore, it was ignored and assumed equal to zero for SH.

Table 1. Calculated values of coupling constants (in cm^{-1}) using DFT methods.

DFT level[1]	J_1	J_2	J_3	J_{12}	J_{13}
B3LYP	157.4	179.5	146.1	−26.6	−26.3
TPSSh	209.6	231.4	188.4	−37.5	−37.3
cam-B3LYP	116.3	137.9	112.3	−17.8	−17.4
LC-BLYP	131.4	155.0	125.6	−25.7	−25.6
wB97m-v	98.2	116.5	95.9	−14.6	−14.4

To clarify and verify the results of DFT calculations, ab initio CASSCF/NEVPT2 computations with partial diamagnetic substitution of paramagnetic centers in **1** were also performed. For this purpose, the Ni^{2+}-centers (M_2 and M_3) were replaced by Zn^{2+} ions in the trinuclear molecule. In addition, the radicals (1 and 2) were also replaced by their reduced analogs 4,4,5,5-tetramethyl-2-(6-methylpyridin-2-yl)-4,5-dihydro-1H-imidazol-1-olhaving a hydroxyl amine moiety, >N-OH, instead of the nitroxyl group >N-O. In this way, a cluster with only one exchange-bonded pair was obtained: Ni^{2+} (S = 1) and imino nitroxyl radical (S = 1/2), respectively (Figure 6). The ground state of such a spin system is a quartet, and the energy gap between the ground state and, nearest to it, the spin doublet can be calculated by the formula: $J_1 = (E(D) - E(Q))/3$. The results of the calculation of J_1 obtained in this way are summarized in Table 2.

 doi:10.20944/preprints202505.2369.v1

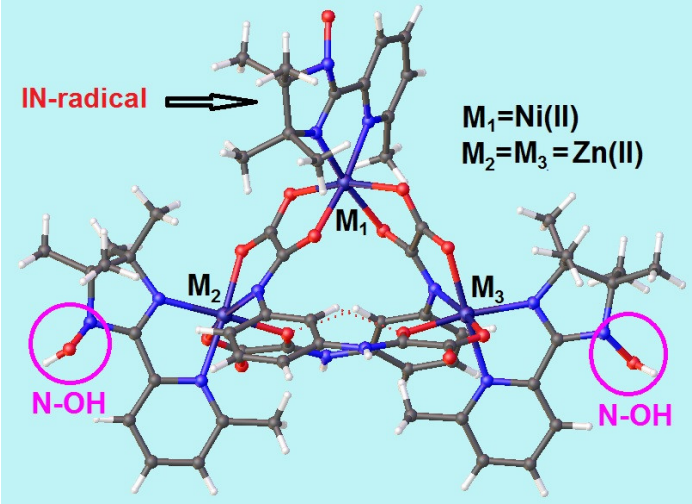

Figure 6. Partial diamagnetic substitution scheme for the calculation of constant J_1, see text.

Table 2. Calculated values of coupling constants (in cm^{-1}) using ab initio methods.

CAS(n,m) roots(*Q*,*D*)	*E*(*Q*)–*E*(*D*) CASSCF	J_1 CASSCF	*E*(*Q*)–*E*(*D*) NEVPT2	J_1 NEVPT2
13,9)/(2, 2)	-95.9	**32.0**	-108.6	**36.2**

[1] Tables may have a footer.

A similar diamagnetic substitution approach (see Figure 7) was implemented for the CASSCF/NEVPT2 computation of the J_{12} exchange integral between Ni^{2+} ions (M_1 and M_2). The constant J_{12} in this case is found by the formula: $J_{12} = (E(T) - E(S))/2$ (see Table 3).

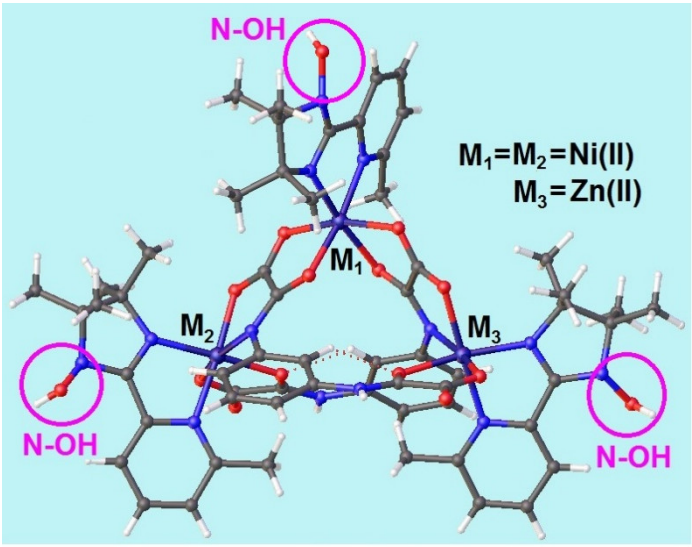

Figure 7. Partial diamagnetic substitution scheme for the calculation of constant J_{12}, see text.

Table 3. Calculated values for energy levels and coupling constant $J_{12} = (E(T) - E(S))/2$ (in cm^{-1}).

CAS(n,m) roots(*Q*,*T*,*S*)	E (Singlet)	*E* (Triplet)	*E*(Quintet)	J_{12}
cas (10,9)/(2,2,2))	0	3.5	10.6	−1.75
NEVPT2	0	7.7	21.3	−3.85

[1] Tables may have a footer.

 doi:10.20944/preprints202505.2369.v1

As evidenced by a comparison the data from the Tables 2 and 3 with those of Table 1, there is a substantial discrepancy between the exchange integral values obtained from DFT calculations and CASSCF/NEVPT2 data, with a range from 4 to 7 times.

To estimate the other SH parameters, the *g*-tensor and *D*-tensor of the paramagnetic center M_1 (Ni^{2+}, S = 1), were calculated using the diamagnetic substitution shown in Figure 5. The results of the computations are summarized in Table 4. Considering the obtained anisotropy of the Ni g-tensor, which is less than 2%, only the isotropic part of the g-tensor is presented in Table 4, in which the parameters corresponding to the standard form of the D tensor along the principal axes are also given.

Table 4. Calculated parameters of g and D tensors for the paramagnetic center M_1 (Ni^{2+}, S = 1).

SH parameter	Method						
	cas(8,5)[1]	NEVPT2[2]	B3LYP[3]	TPSSh[3]	cam-B3LYP[3]	LC-BLYP[3]	wB97m-v[3]
g	**2.29**	2.22	2.17	2.12	2.18	2.15	2.14
D	7.43	4.92	2.49	1.83	**2.01**	8.07	3.20
E/D	0.069	0.087	0.328	0.183	0.297	0.243	0.162

[1]roots(10,9); [2]cas(8,5), roots(10,9); [3]SOMF(1X).

According to the DFT calculations, it was hypothesized that all exchange integral values of Ni–IN are equivalent ($\boldsymbol{J} = \boldsymbol{J}_1 = \boldsymbol{J}_2 = \boldsymbol{J}_3$), as well as $\boldsymbol{J}(Ni_1–Ni_2) = \boldsymbol{J}(Ni_1–Ni_3)$ during the simulation of experimental data on $\chi T(T)$. This approach was adopted to circumvent the issue of over-parameterization. Furthermore, the parameters of the *g*- and *D*-tensors for all Ni-centers were considered equal. The results of the experimental data fitting performed in the Phi program are displayed in Figure 3.

The best fitting parameters are as follows: $g_{Ni} = 2.3$; $D_{Ni} = 2.0$ cm^{-1}; $\boldsymbol{J} = \boldsymbol{J}_1 = \boldsymbol{J}_2 = \boldsymbol{J}_3 = 36.2$ cm^{-1}; $\boldsymbol{J}_{12} = \boldsymbol{J}_{13} = -18.9$ cm^{-1}. These parameters were also used to fit the experimental magnetization data, $M(H)$, registered at a temperature of 2K (see Figure 4).

The comparison of the optimal values for the exchange integrals, g_{Ni} and D_{Ni}, obtained from the $\chi T(T)$ simulation with the results of quantum-chemical calculations (Tables 2-4), shows that the best value for $g_{Ni} = 2.29$ is provided by cas(8,5) calculation. DFT computation, especially cam-B3LYP, most accurately reproduces D_{Ni}. The CAS(13,9)/NEVPT2 method gives a very close value for Ni-IN exchange integral, ***J***, but ab initio approach can't reproduce the $\boldsymbol{J}_{12}$ (Ni_1-Ni_2) exchange integral. The CAM-B3LYP calculation is the most accurate in this case.

The estimation of the magnetic exchange interactions between neighboring hydrogen-bonded triangular molecules of the complex **1** (see Figure 5) obtained from the DFT computation yielded a negative $\boldsymbol{J}_{inter}$, with its absolute value ranging from 0.1 to 0.2 cm^{-1}.

3. Materials and Methods

3.1. Instrumental and Physical Measurements

Elemental (C,H,N) analysis was performed on a Euro-Vector 3000 analyzer (Eurovector, Redavalle, Italy). FTIR spectra were registered with a NICOLET spectrophotometer (Thermo Electron Scientific Instruments LLC, Madison, WI, USA) in the 4000–400 cm^{-1} range. Thermal stability of 1 was studied by means of Thermo Microbalance TG 209 F1 Iris (Netzsch, Selb, Germany). The cryomagnetic investigation of the compound was performed using a Quantum Design MPMS 5XL SQUID magnetometer (Quantum Design, Inc., San Diego, CA, USA) in the temperature range of 1.8–300 K and under a magnetic field of up to 7 T. The diamagnetic contribution for the magnetic susceptibility of the complex **1** was corrected using Pascal's constants for the constituent atoms and organic ligand bonds [38].

 doi:10.20944/preprints202505.2369.v1

Single-crystal XRD experimental details are presented in Table S2 (, SM). Crystallographic data were deposited with the Cambridge Crystallographic Data Centre (deposit number CCDC 2451012).

3.2. Theoretical Calculations

Quantum chemical study was fulfilled using crystallographic geometry. The calculations of magnetic exchange *J* integrals, D tensors, and g tensors was performed by both broken-symmetry DFT (BS-DFT) [39] and ab initio CAS/NEVPT2 methods with def2-QZVPP basis set for Ni and def2-TZVP for other atoms using the Orca-6.0 software package [40,41]. Fitting of the experimental χT(T) and *M*(H) dependences to obtain optimal parameters of employed spin–Hamiltonian was carried out using the PHI 3.16 package [42].

3.3. Preparations

Solvents of the reagent grade (EKOS-1, Moscow, Russia) were distilled prior to use. The complex was synthesized under ambient conditions. The radical 2-(6-methyl-2-pyridyl)-4,4,5,5,5-tetramethylimidazoline-1-oxyl (IN) was synthesized according to a literature procedure [23]. Tritopic derivative, Na_3L, was prepared in situ by hydrolysis of ethyl-2- [3- [(2-ethoxy-2-oxo-acetyl)amino]anilino]-2-oxo-acetate [12].

3.3.1. Synthesis of $[Ni_3(L^{3-})_2(IN)_3]\cdot 5CH_3OH$

The solution 1: Under stirring and heating (80 C), a solution of IN (38 mg, 0.165 mmol) in 1.5 mL H_2O was added dropwise to a solution of $Ni(ClO_4)_2\cdot 6H_2O$ (60 mg, 0.165 mmol) in 2.5 mL H_2O.

The solution 2. The hydrolysis of ethyl-2- [3- [(2-ethoxy-2-oxo-acetyl)amino]anilino]-2-oxoacetate [43,44], the esterified form of 2- [3-(oxaloamino)anilino]-2-oxoacetic acid was performed in 2 mL of distilled water? Which was added to the mixture of ethyl-2- [3- [(2-ethoxy-2-oxo-acetyl)amino]anilino]-2-oxoacetate (33 mg, 0.11 mmol) and NaOH (18 mg, 0.45 mmol). The mixture was then stirred at a magnetic stirrer at a temperature of 80°C for 15 minutes.

An elemental analysis of complex **1** was performed on a desolvated sample that was heated to 110°C until constant weight was reached: Anal Calcd. for $Ni_3C_{59}H_{64}N_{13}O_{15}$ (mass. %): C, 51.74; H, 4.71; N, 13.30; found: C, 51.68; H, 4.6; N, 13.25. IR spectrum (KBr, ν, cm^{-1}): 3400, 3268, 3102, 2965, 2925, 2857, 1717, 1656, 1590, 1472, 1448, 1386, 1335, 1072, 700.

4. Conclusions

Among the complexes of d-metals with phenylene-based bis-oxamate ligands, the compound studied by us is distinguished by its atypical tri-nuclear triangular molecular structure, in which three metal centers are connected by only two anionic bridges, representing a triply deprotonated form of 2- [3-(oxaloamino)anilino]-2-oxoacetic acid, complexes with such a form of the latter having not been previously known.

Despite the presence of six possible magnetic couplings in the trinuclear cluster 1, its magnetic behavior was well reproduced using the three-J model and magnetic anisotropy D under the assumption that three different Ni-IN interactions are equal to each other, and considering only two equivalent Ni-Ni interactions, with the third one equating to zero. This restriction was implemented to circumvent the issue of over parameterization. The magnetic plots simulation results indicate the presence of two opposite in nature types of magnetic interactions within the triangular core. DFT and detailed CASSCF/NEVPT2 computations were also performed, thereby providing support for the experimental modeling of the magnetic data.+

Supplementary Materials: The following supporting information can be downloaded at the website of this paper posted on Preprints.org, Figure S1: title; Table S1: title; Video S1: title.

 doi:10.20944/preprints202505.2369.v1

Author Contributions: For research articles with several authors, a short paragraph specifying their individual contributions must be provided. The following statements should be used "Conceptualization, KEV and VAM; methodology, KEV; software, VAM; validation, KEV, DGS and VAM.; investigation, All; resources, KEV; data curation, DGS; writing—original draft preparation, KEV; writing—review and editing, All; visualization, KEV and DGS; supervision, KEV. All authors have read and agreed to the published version of the manuscript."

Funding: The research was supported by the Ministry of Science and Higher Education of the Russian Federation, N 125020401317-8

Data Availability Statement: CCDC2451012 entry contains the supplementary crystallographic data for this paper. This original data presented in the study are openly available in The Cambridge Crystallographic Data Center at https://www.ccdc.cam.ac.uk/structures/2451012. The original contributions presented in this study are included in the article/Supplementary Materials. Further inquiries can be directed to the corresponding author.

Conflicts of Interest: The authors declare no conflicts of interest

References

1. Bhatt, V.; Ram, S. The Role of Ligands, Polytopic Ligands and Metal Organic Ligands (Mols) in Coordination Chemistry. *Chem. Sci. Rev. Lett.* **2015**, *4*, 414–428.
2. Ruiz, R.; Faus, J.; Lloret, F.; Julve, M.; Journaux, Y. Coordination Chemistry of N,N′-Bis(Coordinating Group Substituted)Oxamides: A Rational Design of Nuclearity Tailored Polynuclear Complexes. *Coord. Chem. Rev.* **1999**, *193–195*, 1069–1117, doi:https://doi.org/10.1016/S0010-8545(99)00138-1.
3. Pardo, E.; Ruiz-García, R.; Cano, J.; Ottenwaelder, X.; Lescouëzec, R.; Journaux, Y.; Lloret, F.; Julve, M. Ligand Design for Multidimensional Magnetic Materials: A Metallosupramolecular Perspective. *Dalt. Trans.* **2008**, 2780, doi:10.1039/b801222a.
4. Dul, M.-C.; Pardo, E.; Lescouëzec, R.; Journaux, Y.; Ferrando-Soria, J.; Ruiz-García, R.; Cano, J.; Julve, M.; Lloret, F.; Cangussu, D.; et al. Supramolecular Coordination Chemistry of Aromatic Polyoxalamide Ligands: A Metallosupramolecular Approach toward Functional Magnetic Materials. *Coord. Chem. Rev.* **2010**, *254*, 2281–2296, doi:https://doi.org/10.1016/j.ccr.2010.03.003.
5. Journaux, Y.; Ferrando-Soria, J.; Pardo, E.; Ruiz-Garcia, R.; Julve, M.; Lloret, F.; Cano, J.; Li, Y.; Lisnard, L.; Yu, P.; et al. Design of Magnetic Coordination Polymers Built from Polyoxalamide Ligands: A Thirty Year Story. *Eur. J. Inorg. Chem.* **2018**, *2018*, 228–247, doi:10.1002/ejic.201700984.
6. Mariano, L. dos S.; Rosa, I.M.L.; De Campos, N.R.; Doriguetto, A.C.; Dias, D.F.; do Pim, W.D.; Valdo, A.K.S.M.; Martins, F.T.; Ribeiro, M.A.; De Paula, E.E.B.; et al. Polymorphic Derivatives of NiII and CoII Mesocates with 3D Networks and "Brick and Mortar" Structures: Preparation, Structural Characterization, and Cryomagnetic Investigation of New Single-Molecule Magnets. *Cryst. Growth Des.* **2020**, *20*, 2462–2476, doi:10.1021/acs.cgd.9b01638.
7. Simões, T.R.G.; do Pim, W.D.; Silva, I.F.; Oliveira, W.X.C.; Pinheiro, C.B.; Pereira, C.L.M.; Lloret, F.; Julve, M.; Stumpf, H.O. Solvent-Driven Dimensionality Control in Molecular Systems Containing CuII, 2,2′-Bipyridine and an Oxamato-Based Ligand. *CrystEngComm* **2013**, *15*, 10165, doi:10.1039/c3ce41783b.
8. Lisnard, L.; Chamoreau, L.-M.; Li, Y.; Journaux, Y. Solvothermal Synthesis of Oxamate-Based Helicate: Temperature Dependence of the Hydrogen Bond Structuring in the Solid. *Cryst. Growth Des.* **2012**, *12*, 4955–4962, doi:10.1021/cg300877r.
9. de Campos, N.R.; Simosono, C.A.; Landre Rosa, I.M.; da Silva, R.M.R.; Doriguetto, A.C.; do Pim, W.D.; Gomes Simões, T.R.; Valdo, A.K.S.M.; Martins, F.T.; Sarmiento, C. V.; et al. Building-up Host–Guest Helicate Motifs and Chains: A Magneto-Structural Study of New Field-Induced Cobalt-Based Single-Ion Magnets. *Dalt. Trans.* **2021**, *50*, 10707–10728, doi:10.1039/D1DT01693H.
10. Francescon, J.E.; de J Pfau, S.C.; Borth, K.W.; Marinho, M.V.; Pedroso, E.F.; Giese, S.O.K.; Pereira, C.L.M.; Miorim, A.J.F.; Maciel, G.M.; Hughes, D.L.; et al. Isomorphic Oxamate Derivatives Triple Mesocates: From the Synthesis to Antibacterial Activities. *J. Mol. Struct.* **2025**, *1328*, 141272, doi:10.1016/j.molstruc.2024.141272.

 doi:10.20944/preprints202505.2369.v1

11. Fernández, I.; Ruiz, R.; Faus, J.; Julve, M.; Lloret, F.; Cano, J.; Ottenwaelder, X.; Journaux, Y.; Muñoz, M.C. Ferromagnetic Coupling through Spin Polarization in a Dinuclear Copper(II) Metallacyclophane. *Angew. Chemie Int. Ed.* **2001**, *40*, 3039–3042, doi:10.1002/1521-3773(20010817)40:16<3039::AID-ANIE3039>3.0.CO;2-P.
12. Pardo, E.; Morales-Osorio, I.; Julve, M.; Lloret, F.; Cano, J.; Ruiz-García, R.; Pasán, J.; Ruiz-Pérez, C.; Ottenwaelder, X.; Journaux, Y. Magnetic Anisotropy of a High-Spin Octanuclear Nickel(II) Complex with a Meso -Helicate Core. *Inorg. Chem.* **2004**, *43*, 7594–7596, doi:10.1021/ic048965x.
13. Pardo, E.; Ruiz-García, R.; Lloret, F.; Julve, M.; Cano, J.; Pasán, J.; Ruiz-Pérez, C.; Filali, Y.; Chamoreau, L.-M.; Journaux, Y. Molecular-Programmed Self-Assembly of Homo- and Heterometallic Penta- and Hexanuclear Coordination Compounds: Synthesis, Crystal Structures, and Magnetic Properties of Ladder-Type Cu II 2 M II x (M = Cu, Ni; x = 3, 4) Oxamato Complexes with Cu II 2 Metall. *Inorg. Chem.* **2007**, *46*, 4504–4514, doi:10.1021/ic062453w.
14. Cangussu, D.; Pardo, E.; Dul, M.-C.; Lescouëzec, R.; Herson, P.; Journaux, Y.; Pedroso, E.F.; Pereira, C.L.M.; Stumpf, H.O.; Carmen Muñoz, M.; et al. Rational Design of a New Class of Heterobimetallic Molecule-Based Magnets: Synthesis, Crystal Structures, and Magnetic Properties of Oxamato-Bridged (M′=LiI and MnII; M=NiII and CoII) Open-Frameworks with a Three-Dimensional Honeycomb Architecture. *Inorganica Chim. Acta* **2008**, *361*, 3394–3402, doi:10.1016/j.ica.2008.02.042.
15. Pardo, E.; Cangussu, D.; Lescouëzec, R.; Journaux, Y.; Pasán, J.; Delgado, F.S.; Ruiz-Pérez, C.; Ruiz-García, R.; Cano, J.; Julve, M.; et al. Molecular-Programmed Self-Assembly of Homo- and Heterometallic Tetranuclear Coordination Compounds: Synthesis, Crystal Structures, and Magnetic Properties of Rack-Type Cu II 2 M II 2 Complexes (M = Cu and Ni) with Tetranucleating Phenylenedioxamato Bridgi. *Inorg. Chem.* **2009**, *48*, 4661–4673, doi:10.1021/ic900055d.
16. Dul, M.-C.; Ottenwaelder, X.; Pardo, E.; Lescouëzec, R.; Journaux, Y.; Chamoreau, L.-M.; Ruiz-García, R.; Cano, J.; Julve, M.; Lloret, F. Ferromagnetic Coupling by Spin Polarization in a Trinuclear Copper(II) Metallacyclophane with a Triangular Cage-Like Structure. *Inorg. Chem.* **2009**, *48*, 5244–5249, doi:10.1021/ic9002274.
17. Pardo, E.; Ferrando-Soria, J.; Dul, M.; Lescouëzec, R.; Journaux, Y.; Ruiz-García, R.; Cano, J.; Julve, M.; Lloret, F.; Cañadillas-Delgado, L.; et al. Oligo- m -phenyleneoxalamide Copper(II) Mesocates as Electro-Switchable Ferromagnetic Metal–Organic Wires. *Chem. – A Eur. J.* **2010**, *16*, 12838–12851, doi:10.1002/chem.201001737.
18. Dul, M.-C.; Lescouëzec, R.; Chamoreau, L.-M.; Journaux, Y.; Carrasco, R.; Castellano, M.; Ruiz-García, R.; Cano, J.; Lloret, F.; Julve, M.; et al. Self-Assembly, Metal Binding Ability, and Magnetic Properties of Dinickel(Ii) and Dicobalt(Ii) Triple Mesocates. *CrystEngComm* **2012**, *14*, 5639, doi:10.1039/c2ce25434d.
19. Oliveira, W.X.C.; Ribeiro, M.A.; Pinheiro, C.B.; da Costa, M.M.; Fontes, A.P.S.; Nunes, W.C.; Cangussu, D.; Julve, M.; Stumpf, H.O.; Pereira, C.L.M. Palladium(II)–Copper(II) Assembling with Bis(2-Pyridylcarbonyl)Amidate and Bis(Oxamate) Type Ligands. *Cryst. Growth Des.* **2015**, *15*, 1325–1335, doi:10.1021/cg5017388.
20. T. da Cunha, T.; X. C. Oliveira, W.; F. Pedroso, E.; Lloret, F.; Julve, M.; L. M. Pereira, C. Heterobimetallic One-Dimensional Coordination Polymers MICuII (M = Li and K) Based on Ferromagnetically Coupled Di- and Tetracopper(II) Metallacyclophanes. *Magnetochemistry* **2018**, *4*, 38, doi:10.3390/magnetochemistry4030038.
21. Wojnar, M.K.; Laorenza, D.W.; Schaller, R.D.; Freedman, D.E. Nickel(II) Metal Complexes as Optically Addressable Qubit Candidates. *J. Am. Chem. Soc.* **2020**, *142*, 14826–14830, doi:10.1021/jacs.0c06909.
22. Tlemsani, I.; Lambert, F.; Suaud, N.; Herrero, C.; Guillot, R.; Barra, A.-L.; Gambarelli, S.; Mallah, T. Assessing the Robustness of the Clock Transition in a Mononuclear S = 1 Ni(II) Complex Spin Qubit. *J. Am. Chem. Soc.* **2025**, *147*, 4685–4688, doi:10.1021/jacs.4c14367.
23. Yamamoto, Y.; Suzuki, T.; Kaizaki, S. Syntheses, Structures, Magnetic, and Spectroscopic Properties of Cobalt(Ii), Nickel(Ii) and Zinc(Ii) Complexes Containing 2-(6-Methyl)Pyridyl-Substituted Nitronyl and Imino Nitroxide†. *J. Chem. Soc. Dalt. Trans.* **2001**, 2943–2950, doi:10.1039/b103647p.
24. Higashikawa, H.; Inoue, K.; Maryunina, K.Y.; Romanenko, G. V.; Bogomyakov, A.S.; Kuznetsova, O. V.; Fursova, E.Y.; Ovcharenko, V.I. Synthesis, Structure and Magnetic Properties of the Pentanuclear Complex

 doi:10.20944/preprints202505.2369.v1

[Fe2(CN)12Ni3(L)6]·27H2O, Where L Is Nitronyl Nitroxide. *J. Struct. Chem.* **2009**, *50*, 1155–1158, doi:10.1007/s10947-009-0169-x.

25. Kuznetsova, O. V.; Romanenko, G. V.; Letyagin, G.A.; Bogomyakov, A.S. Binuclear Co(II), Ni(II), and Cu(II) Hexafluoroacetylacetonates with Spin-Labeled Nitrophenols. *J. Struct. Chem.* **2023**, *64*, 1470–1481, doi:10.1134/S0022476623080115.
26. Ovcharenko, V.; Kuznetsova, O.; Fursova, E.; Letyagin, G.; Romanenko, G.; Bogomyakov, A.; Zueva, E. Simultaneous Introduction of Two Nitroxides in the Reaction: A New Approach to the Synthesis of Heterospin Complexes. *Inorg. Chem.* **2017**, *56*, 14567–14576, doi:10.1021/acs.inorgchem.7b02308.
27. Luneau, D.; Rey, P.; Laugier, J.; Belorizky, E.; Cogne, A. Ferromagnetic Behavior of Nickel(II)-Imino Nitroxide Derivatives. *Inorg. Chem.* **1992**, *31*, 3578–3584, doi:10.1021/ic00043a018.
28. Vostrikova, K.E.; Luneau, D.; Wernsdorfer, W.; Rey, P.; Verdaguer, M. A S = 7 Ground Spin-State Cluster Built from Three Shells of Different Spin Carriers Ferromagnetically Coupled, Transition-Metal Ions and Nitroxide Free Radicals. *J. Am. Chem. Soc.* **2000**, *122*, 718–719, doi:10.1021/ja993210o.
29. Tsukahara, Y.; Kamatani, T.; Iino, A.; Suzuki, T.; Kaizaki, S. Synthesis, Magnetic Properties, and Electronic Spectra of Bis(β-Diketonato)Chromium(III) and Nickel(II) Complexes with a Chelated Imino Nitroxide Radical: X-Ray Structures of [Cr(AcaMe)2(IM2py)]PF6 and [Ni(Acac)2(IM2py)]. *Inorg. Chem.* **2002**, *41*, 4363–4370, doi:10.1021/ic011282m.
30. Babailov, S.P.; Peresypkina, E. V.; Journaux, Y.; Vostrikova, K.E. Nickel(II) Complex of a Biradical: Structure, Magnetic Properties, High NMR Temperature Sensitivity and Moderately Fast Molecular Dynamics. *Sensors Actuators B Chem.* **2017**, *239*, 405–412, doi:10.1016/j.snb.2016.08.015.
31. Hayakawa, K.; Shiomi, D.; Ise, T.; Sato, K.; Takui, T. Stable Iminonitroxide Biradical in the Triplet Ground State. *Chem. Lett.* **2004**, *33*, 1494–1495, doi:10.1246/cl.2004.1494.
32. Zhi-Liang, L.; Li-Cun, L.; Dai-Zheng, L.; Zong-Hui, J.; Shi-Ping, Y.; Zhi-Liang, L.; Li-Cun, L.; Dai-Zheng, L.; Zong-Hui, J.; Shi-Ping, Y. Exchange Interaction of a Novel Heterospin Polynuclear Complex Containing Transition Metals and Imino Nitroxide Radicals: { [(CuL)Nid (IM-2Py) 2] (C10 4) 2 } 2 ·2H 2 O. *Chinese J. Chem.* **2003**, *21*, 133–138, doi:10.1002/cjoc.20030210210.
33. Oshio, H.; Yamamoto, M.; Ito, T.; Kawauchi, H.; Koga, N.; Ikoma, T.; Tero-Kubota, S. Experimental and Theoretical Studies on Ferromagnetically Coupled Metal Complexes with Imino Nitroxides. *Inorg. Chem.* **2001**, *40*, 5518–5525, doi:10.1021/ic0102384.
34. Petrov, P.A.; Romanenko, G. V.; Shvedenkov, Y.G.; Ikorskii, V.N.; Ovcharenko, V.I.; Reznikov, V.A.; Sagdeev, R.Z. Complexes of Cu II, Ni II, and Co II with 2-Cyano-2-(1-Oxyl-4,4,5,5-Tetramethyl-4,5-Dihydro-1H-Imidazol-2-Yl)-1-R-Ethylenolates. *Russ. Chem. Bull.* **2004**, *53*, 99–108, doi:10.1023/B:RUCB.0000024836.23456.a8.
35. Yamamoto, Y.; Suzuki, T.; Kaizaki, S. Crystal Structures, Magnetic and Spectroscopic Properties of Manganese(II), Cobalt(II), Nickel(II) and Zinc(II) Dichloro Complexes Bearing Two 2-Pyridyl-Substituted Imino Nitroxides †. *J. Chem. Soc. Dalt. Trans.* **2001**, 1566–1572, doi:10.1039/b010243l.
36. Kuznetsova, O. V.; Romanenko, G. V.; Bogomyakov, A.S.; Ovcharenko, V.I. Synthesis, Structure, and Magnetic Properties of Heterospin Polymers MI [MII(Hfac)L2]. *Russ. J. Coord. Chem.* **2020**, *46*, 521–527, doi:10.1134/S1070328420070039.
37. Spek, A.L. CheckCIF Validation ALERTS: What They Mean and How to Respond. *Acta Crystallogr. Sect. E Crystallogr. Commun.* **2020**, *76*, 1–11, doi:10.1107/S2056989019016244.
38. Bain, G.A.; Berry, J.F. Diamagnetic Corrections and Pascal's Constants. *J. Chem. Educ.* **2008**, *85*, 532, doi:10.1021/ed085p532.
39. Shoji, M.; Koizumi, K.; Kitagawa, Y.; Kawakami, T.; Yamanaka, S.; Okumura, M.; Yamaguchi, K. A General Algorithm for Calculation of Heisenberg Exchange Integrals J in Multispin Systems. *Chem. Phys. Lett.* **2006**, *432*, 343–347, doi:10.1016/j.cplett.2006.10.023.
40. Neese, F.; Wennmohs, F.; Becker, U.; Riplinger, C. The ORCA Quantum Chemistry Program Package. *J. Chem. Phys.* **2020**, *152*, doi:10.1063/5.0004608.
41. Neese, F. Software Update: The ORCA Program System—Version 5.0. *WIREs Comput. Mol. Sci.* **2022**, *12*, e1606, doi:10.1002/wcms.1606.

 doi:10.20944/preprints202505.2369.v1

42. Chilton, N.F.; Anderson, R.P.; Turner, L.D.; Soncini, A.; Murray, K.S. PHI: A Powerful New Program for the Analysis of Anisotropic Monomeric and Exchange-coupled Polynuclear d - and f -block Complexes. *J. Comput. Chem.* **2013**, *34*, 1164–1175, doi:10.1002/jcc.23234.
43. Wright, J.B.; Hall, C.M.; Johnson, H.G. N,N′-(Phenylene)Dioxamic Acids and Their Esters as Antiallergy Agents. *J. Med. Chem.* **1978**, *21*, 930–935, doi:10.1021/jm00207a016.
44. Blay, G.; Fernández, I.; Pedro, J.R.; Ruiz-García, R.; Muñoz, M.C.; Cano, J.; Carrasco, R. A Hydrogen-Bonded Supramolecular Meso-Helix. *European J. Org. Chem.* **2003**, *2003*, 1627–1630, doi:10.1002/ejoc.200200544.